Nucleation-free 3D rigidity

Jialong Cheng[1], Meera Sitharam[1] and Ileana Streinu[2]

Abstract

All known examples of generic 3D bar-and-joint frameworks where the distance between a non-edge pair is implied by the edges in the graph contain a rigid vertex-induced subgraph.

In this paper we present a class of arbitrarily large graphs with no non-trivial vertex-induced rigid subgraphs, which have implied distances between pairs of vertices not joined by edges. As a consequence, we obtain (a) the first class of counter-examples to a potential combinatorial characterization of 3D generic independence and rigidity proposed by Sitharam and Zhou [5] and (b) the first example of a 3D rigidity circuit which has no non-trivial rigid induced subgraphs.

1 Introduction

Finding a combinatorial characterization for rigidity and independence of bar-and-joint frameworks in 3D remains an elusive, long-standing open problem. In 2D, the question is completely answered by Laman's Theorem, with several other equivalent characterizations (e.g. [4]) leading to efficient algorithms.

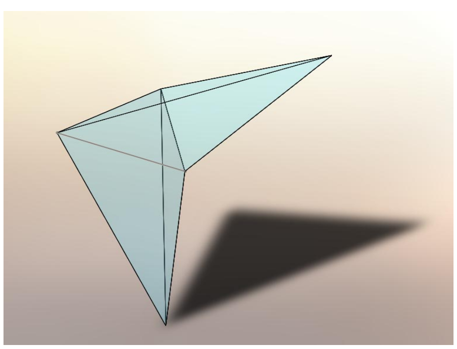

Figure 1: A banana-framework.

Laman's Theorem. *The graph $G = (V, E)$ underlying a bar-and-joint framework $G(p)$ is independent in 2D if and only if every subgraph $G' = (V', E')$ of G satisfies the edge-sparsity counts $|E'| \leq 2|V'| - 3$.*

We refer the reader to [3] for standard terminology and notations in Rigidity Theory.

A generalization of this condition, originating in James Clerk Maxwell's work from the 19th century, is known to be necessary, but not sufficient for 3D independence, resp. rigidity:

Maxwell's Counting Condition. A graph G satisfies Maxwell's counts in 3D if all its subgraphs $G' = (V', E')$ span at most $|E'| \leq 3|V'| - 6$ edges.

In addition, *minimally rigid* graphs in 3D must have exactly $|E| = 3|V| - 6$ edges. A simple example of a rigid graph, obviously satisfying these counts, is the *banana* framework from Fig. 1, obtained by glueing together the skeleta of two 3D tetrahedra.

However, it is known that Maxwell's condition is not sufficient. The classical example (the so-called *double-banana graph*) is illustrated in Fig. 2. It satisfies Maxwell's counts, but the framework is clearly flexible, and dependent. Intuitively, the dependence arises as follows.

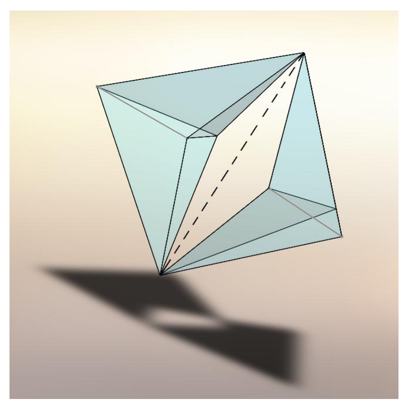

Figure 2: The *double-banana* framework.

A *non-edge* of G is a pair $(u, v) \notin E$. A non-edge is said to be *implied* if there exists an independent subgraph G' of G such that $G' \cup (u, v)$ is dependent. This is equivalent to saying that there is no infinitesimal motion with a non-zero component along the direction of $p(u) - p(v)$, in a generic realization $G(p)$ of G.

The non-edge shared by the two bananas is *implied*, in G, by each of its banana subgraphs. Since each banana is rigid, as an induced subgraph, the distance along the non-edge (u, v) (along which the bananas are connected) is double-determined, and the graph is *dependent*.

[1]Department of CISE, University of Florida, Gainesville, FL, USA. Research supported by NSF CISE/CCF 0622106 and NSF DMS/NIGMS 0714912, and by a research gift from Solidworks. {jicheng,sitharam}@cise.ufl.edu

[2]Department of Computer Science, Smith College, Northampton, MA 01063, USA. istreinu@smith.edu,http://cs.smith.edu/~streinu. Research supported by NSF CCF-0728783 and by a DARPA "23 Mathematical Challenges" grant.

Other frameworks, such as the *triple-banana* of Fig. 3, may contain *rigid components* made entirely from implied non-edges. These components would not be rigid as induced subgraphs. Another example of a dependent graph satisfying Maxwell's counts for independence is due to Crapo (Fig. 4).

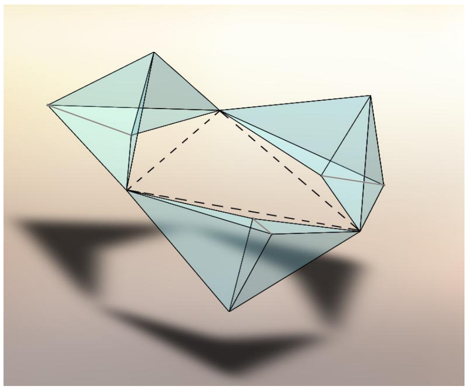

Figure 3: The *triple-banana* framework. Besides the three bananas, a fourth rigid component is induced by the three implied non-edges (dashed).

These examples, as well as all known counterexamples to Maxwell's counts [2] appearing in the literature satisfy the following:

Nucleation property. A graph G has the *nucleation property* if it contains a non-trivial rigid induced subgraph. *Trivial* means a complete graph on 4 or fewer vertices.

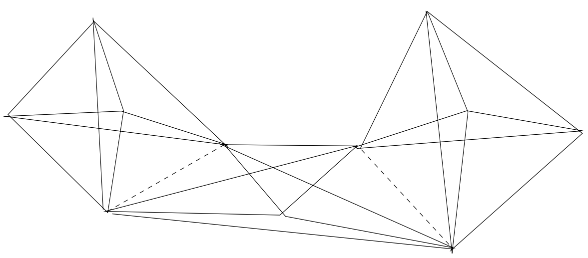

Figure 4: Crapo's graph with a "hinge" structure

This leads to the natural question:

Nucleation-free Rigid Graphs: *Do all graphs that are dependent but satisfy Maxwell's counts have the nucleation property?*

Our Contribution. We answer this question in the negative. We construct a class of flexible 3D frameworks satisfying Maxwell's counts which have no proper rigid nuclei besides trivial ones (triangles).

Further consequences. Sitharam and Zhou [5] gave several examples where Maxwell's counts were insufficient for rigidity, all of which satisfy the nucleation property. Using a combinatorial notion capturing the recursive nature of nucleation (called *module-rigidity*), they propose an algorithm which characterizes generic independence in a large class of such graphs by using the presence of rigid nuclei. It has been an open problem whether this algorithm can fail to detect 3D independence and rigidity, i.e. whether module-rigidity coincides or not with 3D rigidity.

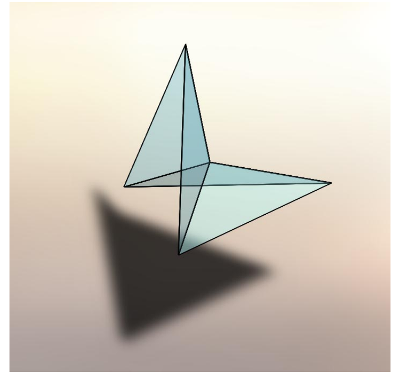

Figure 5: A roof.

The result presented here settles the question (in the negative).

As another consequence of our work, we obtain the first example of a flexible 3D rigidity circuit which has no non-trivial rigid induced subgraph. Until now, such examples were only available in 4D, but, according to [3], not in 3D: *The only known non-rigid circuits in the 3D rigidity matroid arise from amalgamations of circuits forced by Maxwell's condition.* In 2D, however, all rigidity circuits are rigid. Our result implies, in addition, that Lovasz' characterization [4] of 2D rigidity via *coverings* cannot be extended to 3D.

In the rest of this abstract we describe the counter-examples and sketch the proofs.

2 Main example: a ring of 7 roofs

We define a *roof* to be a graph obtained from K_5, the complete graph of five vertices, by deleting two non-adjacent edges. A 3D realization of a roof is depicted in Fig. 5. In the terminology of [7], this is a *single-vertex origami* over a 4-gon.

The basis of our family of counter-examples is the ring of 7 roofs. Two roofs are connected along a non-edge, as in Fig. 6. Since there are only two edges that were removed from K_5, each roof can be connected to at most two others. A chain of seven roofs is closed back into a ring, as depicted schematically in Fig. 7. It is trivial to see that this graph contains no non-trivial induced rigid subgraph. It remains to show that each roof is a rigid component in the context of the entire ring. The

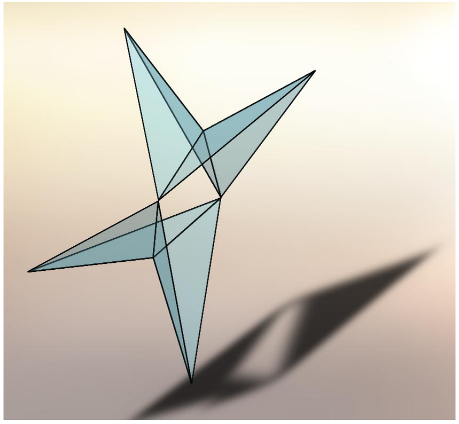

Figure 6: Connecting two roofs.

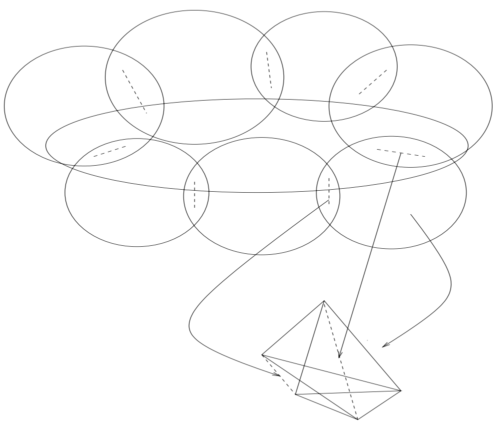

Figure 7: R_7. In this graph, each circle represents a roof, which has two hinges denoted as dotted lines, and the oval represents the ring.

proof proceeds by showing that each roof's non-edges are *implied*.

The main theorem and two of its important corollaries can now be stated.

Theorem 1 *In a ring of 7 roofs, the two non-edges within each individual roof are implied.*

The proof will be sketched in the next section.

Corollary 2 *The double-ring of 7 roofs from Fig. 8 answers the Nucleation-Free Rigid Graph Question in the negative.*

Proof. From Theorem 1 it follows that both the left and the right rings of Fig. 8 imply the non-edge (u, v). Hence both rings determine the distance of (u, v), and the double-ring is generically dependent. However, since the entire graph has no non-trivial rigid induced subgraphs, it does not have the Nucleation Property. It is easy to verify that it satisfies Maxwell's sparsity counts. The double 7-ring has 3dofs. This can be easily observed by counting: each 7-ring has 1dof, and there is an additional rotation along the multiple non-edge hinge where the two rings are glued. □

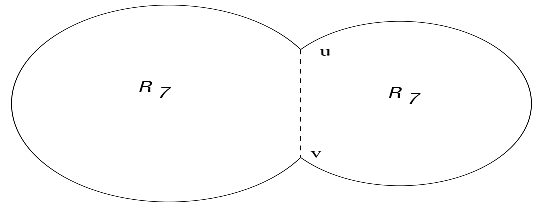

Figure 8: The double-ring of 7 roofs, obtained by glueing two rings along a roof non-edge.

Corollary 3 *On the flexible double-ring in Fig. 9, the algorithm of [5] returns* module-rigid. *Therefore, module-rigidity does not coincide with 3D rigidity.*

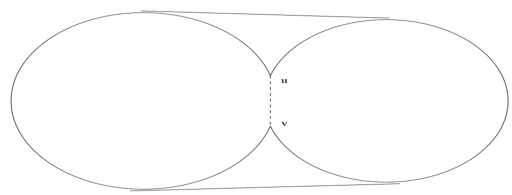

Figure 9: A schematic representation of the 1dof flexible framework that Sitharam and Zhou's[5] algorithm will classify as module-rigid. It is obtained by adding two bars between the two rings of the double-ring of Fig. 8.

Proof. When a graph has no smaller induced rigid subgraphs, Sitharam and Zhou's[5] algorithm reduces to checking Maxwell's counts. In this case, the graph will be declared module-rigid. On the other hand, it has one degree of dependency, and hence one degree of freedom, since (u, v) is an implied edge. Another way of seeing this is to observe that the two extra bars can only eliminate two dofs from the 3dofs double-ring. This shows that module-rigidity is a weaker concept than 3D rigidity. □

Corollary 4 *Theorem 1 can be extended to a ring of an arbitrary number $k \geq 7$ of roofs.*

This is a consequence of the *proof* of Theorem 1, and is presented in the next section.

3 Proof of the Main Theorem

We have two proofs, each one relying on a different technique and hence of independent interest. The common denominator is the general approach of proving generic independence by providing an explicit *realization* where the rank of the rigidity matrix associated to a graph is maximum.

In the first proof, we first show, by induction on k, that, generically, the rigidity matrix of a ring of $k \geq 7$ roofs has maximal rank equal to the number of edges (its rows are independent). Therefore this rank is exactly $k-6$ less than the required Maxwell count for rigidity, and thus the ring has, generically, $k-6$ internal degrees of freedom (dofs). Next we show that in any generic realization of the ring, when any one of the non-edges is added to any single roof, the resulting *banana* is rigid. Finally, we use Tay's theorem [8, 9] on body-and-hinge structures to show that the ring, *with these non-edges replaced by edges*, continues to have $k-6$ dofs. This means that the non-edges were implied.

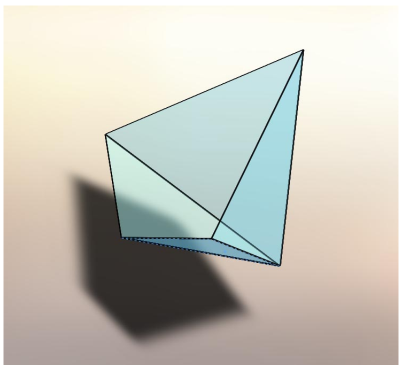

Figure 10: A convex roof. Its two non-edges cannot move simultaneously in an expansive (resp. contractive) fashion.

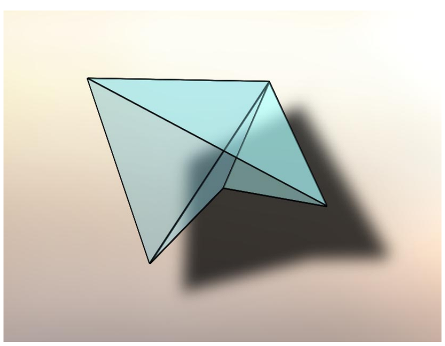

Figure 11: A pointed pseudo-triangular roof. Its two non-edges move simultaneously in either an expansive or contractive fashion.

We sketch now the second proof. It relies on the infinitesimal properties of single-vertex origamis from [7], together with expansion/contraction properties of convex polygons [1] and pointed pseudo-triangulations [6], applied to the simplest possible case of a 4-gon. They imply that the roof realizations from Fig. 10 and 11 have the expansion/contraction properties stated in the captions. We create a realization of a 7-ring by glueing together six pointed pseudo-triangular roofs and one convex roof (we give it explicitly). More generally, for any ring of more than 7 roofs we show the existence of a generic realization in which each non-edge used in glueing two roofs is implied. We remark that, if non-edges within each roof are implied for *one* generic realization, then they are implied for *all* generic realizations.

Lemma 5 *For all odd rings of $2k$, $k \leq 3$ pseudo-triangular roofs and one convex roof, and for all even rings of $2k-3$, $k \geq 4$ pseudo-triangular and 3 convex roofs, the glueing non-edges are implied.*

Proof. The increase/decrease patterns of the two non-edges for the roofs are: "both expansive" (for the pseudo-triangular case), and "one expansive, one contractive" (for the convex case). Assume that there exists an infinitesimal motion that changes the length of one glueing non-edge, and without loss of generality assume the expanding direction of the motion. When followed along the ring back to the starting non-edge, the patterns imply that the motion must go there in the reverse order (decreasing), a contradiction. □

This concludes the proofs.

Acknowledgement. This work was initiated at the Workshops on *Rigidity and Enumeration* and *Geometric Constraint Systems*, organized by the last author at the Bellairs Research Institute of McGill University in Barbados in 2008 and 2009.

References

[1] R. Connelly. Rigidity and energy. *Inventiones Mathematicae*, 66:11–33, 1982.

[2] H. Crapo. The tetrahedral-octahedral truss. *Structural Topology*, 7:51–60, 1982.

[3] J. Graver, B. Servatius, and H. Servatius. *Combinatorial rigidity*. Graduate Studies in Mathematics. American Mathematical Society, 1993.

[4] L. Lovász and Y. Yemini. On generic rigidity in the plane. *SIAM J. Algebraic and Discrete Methods*, 3(1):91–98, 1982.

[5] M. Sitharam and Y. Zhou. A tractable, approximate characterization of combinatorial rigidity in 3d. In *Abstract 5th Automated Deduction in Geometry (ADG)*, 2004. http://www.cise.ufl.edu/~sitharam/module.pdf.

[6] I. Streinu. Pseudo-triangulations, rigidity and motion planning. *Discrete and Computational Geometry*, 34(4):587–635, 2005.

[7] I. Streinu and W. Whiteley. Single-vertex origami and spherical expansive motions. In *Proc. Japan Conf. Discr. and Comput. Geometry (JCDCG 2004)*, pages 161–173. Springer Verlag, 2005.

[8] T.-S. Tay. Rigidity of multigraphs I: linking rigid bodies in n-space. *Journal of Combinatorial Theory, Series B*, 26:95–112, 1984.

[9] N. White and W. Whiteley. The algebraic geometry of bar-and-body frameworks. *SIAM Journal of Algebraic Discrete Methods*, 8:1–32, 1987.